NACA

RESEARCH MEMORANDUM

EFFECTS OF SWEEP ON THE DAMPING-IN-ROLL CHARACTERISTICS OF THREE SWEPTBACK WINGS HAVING AN ASPECT RATIO OF 4 AT TRANSONIC SPEEDS

By Vernard E. Lockwood

Langley Aeronautical Laboratory
Langley Air Force Base, Va.

NATIONAL ADVISORY COMMITTEE FOR AERONAUTICS
WASHINGTON
December 14, 1950

NATIONAL ADVISORY COMMITTEE FOR AERONAUTICS

RESEARCH MEMORANDUM

EFFECTS OF SWEEP ON THE DAMPING-IN-ROLL CHARACTERISTICS OF THREE SWEPTBACK WINGS HAVING AN ASPECT RATIO OF 4 AT TRANSONIC SPEEDS

By Vernard E. Lockwood

SUMMARY

The damping-in-roll characteristics of three wings having an aspect ratio of 4, a taper ratio of 0.6, an NACA 65A006 airfoil section, and sweep angles of 0°, 35°, and 45° have been determined through a Mach number range from 0.6 to 1.15 and an angle-of-attack range from 0° to approximately 7°. The data were obtained from the Langley 7- by 10-foot tunnel transonic bump by utilizing the twisted-wing technique.

The damping in roll showed a variation with Mach number similar to that of the lift-curve slope; that is, an increase in magnitude of the damping with increase in Mach number in the subsonic range was followed by an appreciable loss through a Mach number of 1.0. Positive damping (negative damping coefficient) was evident for all conditions investigated. At all Mach numbers the damping decreased with increase in sweep angle and at subsonic Mach numbers the variation with sweep was similar to that predicted by theory. The results of the present investigation agreed quantitatively with the results of a free-roll investigation at subsonic Mach numbers on a series of similar wings.

INTRODUCTION

One phase of the National Advisory Committee for Aeronautics transonic research program has been the determination of the control characteristics of flap-type controls throughout the transonic-speed range. The basic control data for a series of wings of aspect ratio 4 are reported in references 1 to 4. In order to determine the rolling effectiveness of these controls, knowledge of the damping in roll of the wings throughout the speed range is necessary. There have been theoretical approaches made to the problem at subsonic speeds (reference 5) and at supersonic speeds (reference 6). These theories do not apply rigidly in the immediate vicinity of $M = 1$; therefore, experimental studies are required to provide the needed data in this speed range. The effects of sweep on the damping-in-roll characteristics have been determined experimentally at high subsonic speeds for one series of wings (reference 7). The available experimental data on the damping-in-roll characteristics in the transonic-speed range are given in references 8 to 12, but these data are mainly for unswept wings at zero lift.

The present paper presents the results of an experimental investigation of the damping-in-roll characteristics of three wings of aspect ratio 4.0 and taper ratio 0.6 with quarter-chord sweep angles of 0°, 35°, and 45°. The investigation utilized linearly twisted semispan wings to represent rolling wings. This method assumes that the rolling moment resulting from a linear variation of angle of attack along the span of the model is equal to the damping moment of an untwisted wing in steady roll. Use of this method with semispan models requires comparison of the test results from twisted and untwisted wings to determine the moments resulting from twist. The damping of a complete wing at any angle of attack is then obtained by combining the rolling moments of both the positive and negative angles of attack of the half-wing.

The tests were made through an angle-of-attack range from 0° to approximately $\pm 7^\circ$ and a Mach number range from 0.60 to 1.15 utilizing the transonic bump of the Langley 7- by 10-foot tunnel. The results are compared at subsonic speeds with experimental results obtained by the use of the free-roll technique on a series of similar wings.

COEFFICIENTS AND SYMBOLS

C_l rolling-moment coefficient at plane of symmetry $\left(\frac{\text{Rolling moment of semispan model}}{qSb}\right)$

R Reynolds number of wing based on $\bar{c}$

$\bar{c}$ mean aerodynamic chord of wing (using theoretical tip), 0.1805 feet $\left(\frac{2}{S}\int_0^{b/2} c^2 dy\right)$

c local wing chord, feet

S twice wing area of semispan model, 0.125 square foot

b twice span of semispan model, 0.7072 foot

y	spanwise distance from plane of symmetry, feet
C_{l_p}	damping-in-roll coefficient $\left(\Delta C_l \dfrac{2V}{pb}\right)$
q	effective dynamic pressure over span of model, pounds per square foot $\left(\frac{1}{2}\rho V^2\right)$
ΔC_l	increment in rolling-moment coefficient caused by wing twist
$pb/2V$	wing twist at tip; equivalent to wing-tip helix angle of a rolling wing, radians
p	rate of roll, radians per second
V	airspeed, feet per second
ρ	mass density of air, slugs per cubic feet
α	angle of attack, degrees
Λ	angle of sweep of wing quarter-chord line, degrees
M	effective Mach number over span of model $\left(\frac{2}{S}\int_0^{b/2} cM_a dy\right)$
M_a	average chordwise local Mach number
M_l	local Mach number
C_{L_α}	lift-curve slope, per degree

MODEL AND APPARATUS

The semispan models used in the investigation had quarter-chord sweep angles of 0°, 35°, and 45°, the wings had an aspect ratio of 4.0, taper ratio of 0.6, and an NACA 65A006 airfoil section parallel to the free stream. The pertinent dimensions of the basic wings are given in figure 1. A typical model setup is shown by the general arrangement of the unswept wing in figure 2. The quarter-chord station of the wing mean aerodynamic chord was always located on the balance center line, and the nose of the fuselage at 7.07 inches ahead of the center line. The ordinates of the fuselage of fineness ratio 10 can be found in table I of reference 3. The unswept wing and the 45° swept wing were made of steel surfaced with bismuth-tin alloy while the 35° swept wing was machined of solid steel. The fuselage was machined of brass.

Two wings were constructed for each sweep angle investigated. One wing was constructed with a linear variation of twist along the span of the model and the other wing was constructed with no twist in order to provide a basis for determining the amount of damping moment due to twist. The measured twist variation along the span of the model is shown in figure 3.

The model was mounted on an electrical strain-gage balance enclosed in the transonic bump, and the rolling moments about the plane of symmetry of the model were indicated by a calibrated potentiometer.

TESTS

The models were tested in the Langley high-speed 7- by 10-foot tunnel utilizing the flow field over the transonic bump to obtain Mach numbers from 0.6 to 1.15. Typical contours of local Mach number in the vicinity of the model location on the bump are shown in figure 4. The contours indicate that there is a Mach number variation of about 0.05 over the model semispan at low Mach numbers and from 0.07 to 0.08 at higher Mach numbers. The chordwise variation is generally less than 0.02. No attempt has been made to evaluate the effects of this chordwise and spanwise Mach number variation. The long-dash lines near the root of the wing in figure 4 indicate a local Mach number 5 percent below the maximum value and represent the estimated extent of the bump boundary layer. The effective test Mach number was obtained from contour charts similar to those presented in figure 4 using the relationship

$$M = \frac{2}{S} \int_0^{b/2} c M_a dy$$

The variation of mean Reynolds number with test Mach number shown in figure 5 is considered typical for the three wings.

CORRECTIONS

Reflection-plane correction factors, which account for the carry-over of load to the other wing, have been applied to the data throughout the Mach number range tested. The correction factors K which were applied are given in figure 6. The values of the correction factor were obtained from an unpublished theoretical investigation. Although the corrections are based on incompressible conditions, it is believed that the results obtained by applying the corrections would give a better representation of true conditions than uncorrected data. Application of the factor K to the data in the manner given results in the values of C_{l_p} being undercorrected at subcritical Mach numbers and probably overcorrected in the transonic Mach numbers ($M > 0.95$).

No corrections were applied for any twisting or deflection of the wing caused by air load. Any bending or twisting as a result of change in angle of attack would not appreciably affect the results of the investigation as it would affect twisted and untwisted wings in a similar manner. The twisted wings, however, could experience an additional twist as a result of the load due to twist. Static loading of the 45° swept wing to approximate the maximum load due to twist indicated a small angular deflection corresponding to a value of $pb/2V$ of 0.004 which is within the accuracy of the investigation. Twisting on the other two wings would be less because of the the smaller sweep angles involved and because the 35° wing is more rigid.

REDUCTION OF DATA

In determining the damping of a wing in roll from a twisted wing, the assumption is made that the damping moment of a steady rolling wing will be equal to the increment in the rolling moment resulting from a linear variation of twist along the span. The assumption that a rolling wing is represented by a wing with a linear twist distribution along the span neglects (1) the increment in dynamic pressure produced by the rolling velocity, and (2) the boundary-layer flow due to the centrifugal force. The error in C_{l_p} resulting from using only the free-stream dynamic pressure is small, about 1 percent. Since the values of $pb/2V$, represented by the twist in the wings, were relatively small, the boundary-layer flow was neglected.

The damping coefficient for the semispan wing was evaluated from the following equation:

$$C_{l_p} = \Delta C_l \frac{2V}{pb} K$$

where

$\Delta C_l = C_{l_{twisted}} - C_{l_{untwisted}}$

$\frac{pb}{2V}$ wing twist at tip, radians

K reflection-plane correction factor

Typical examples of the damping-in-roll coefficients evaluated by the above equation are shown in figure 7 as a function of angle of attack for a semispan wing. The positive angle-of-attack range represents a down-going right wing, whereas the negative angle-of-attack range represents an up-going left wing. The damping coefficient of a complete wing at an angle of attack is, therefore, the sum of the values of C_{l_p} at plus and minus the given angle of attack.

RESULTS AND DISCUSSION

The experimental variation of damping-in-roll parameter C_{l_p} with angle of attack is shown in figure 8 for several Mach numbers. For each of the three wings investigated, the damping coefficient showed an increase with angle of attack up to about 5° for most of the Mach number range. This increase of C_{l_p} with α has been noted previously on a series of similar wings (reference 7). Above $\alpha = 5^{\circ}$, there are indications of large reductions in damping, particularly at the subsonic Mach numbers. Such results may be caused by the nonlinear variation of lift with angle of attack. A study of the effect of nonlinear lift characteristics has been made in reference 13 and has indicated that this effect alone can cause large changes in C_{l_p}.

The results indicate a reduction in damping with increase in sweepback throughout the Mach number range investigated (fig. 9). In general, the loss in damping was more pronounced for sweeps greater than 35°. The data, like those of reference 7, show close agreement between theory and experiment for all sweep angles at $M = 0.6$ and only for the largest sweep angle for $M = 0.85$.

The damping in roll for all the models tested showed an increase in magnitude with Mach number in the subsonic range followed by an appreciable loss through a Mach number of 1.0. (See fig. 10.) Positive damping was evident for all conditions investigated. In general, the variation of C_{l_p} with Mach number was similar to the variation with Mach number of the lift-curve slope which is expressed in figure 11 as the ratio of C_{l_α} at any Mach number to the value of C_{l_α} at $M = 0.6$. (The slopes were measured near zero lift coefficient.)

The similarity in the variation of C_{L_α} and C_{l_p} with M leads to the following simple empirical method of estimating C_{l_p}, if the variation of C_{L_α} with M is available:

$$\left(C_{l_p}\right)_M = \left(C_{l_p}\right)_{M=0.6} \frac{\left(C_{L_\alpha}\right)_M}{\left(C_{L_\alpha}\right)_{M=0.6}}$$

The values of $\left(C_{l_p}\right)_{M=0.6}$ may be either obtained experimentally or estimated by the method of reference 5. (The value of $M = 0.6$ was arbitrarily chosen.) A comparison is given in figure 12 for $\alpha = 0^\circ$ of the estimated values of C_{l_p} obtained by the preceding equation and the results obtained experimentally; the comparison shows that the empirical relationship is useful in the vicinity of $M = 1$, where the existing theoretical relationships do not apply.

A comparison is given in figure 13 of the values of C_{l_p} obtained in the present investigation and the results obtained from free-roll tests on three wings of similar plan form (reference 7). (These wings were geometrically the same with the exception of the quarter-chord sweep angles which were 3.6°, 32.6°, and 46.7° as compared with 0°, 35°, and 45° for the models of the present investigation.) The results of the present investigation are in general agreement with the results of reference 7 at low angles of attack; namely, $\alpha = 0.30^\circ$ and 3.45°. At $\alpha = 6.50^\circ$, there is considerable discrepancy in the data from the two sources. The bump data show much lower values of C_{l_p} than the data of reference 7. This difference may be caused by a Reynolds number effect. A comparison made in reference 14 shows that the lift-curve slope from the larger sting-supported model is essentially unchanged up to $\alpha = 6.5^\circ$; whereas the lift-curve slope of the smaller bump model is materially decreased in the vicinity of $\alpha = 6.5^\circ$. Since C_{l_p} is primarily dependent on C_{L_α}, it would be expected that the values of C_{l_p} obtained on the small bump models would be lower than those obtained on the larger models.

CONCLUDING REMARKS

An investigation of the damping-in-roll characteristics of a series of swept wings of aspect ratio 4 through a Mach number range from 0.6 to 1.15 showed a variation with Mach number similar to that of the lift-curve slope; that is, an increase in magnitude of the damping with increase in Mach number in the subsonic range was followed by an appreciable loss through a Mach number range 1.0. Positive damping was evident for all conditions investigated. At all Mach numbers the damping decreased with increase in sweep angle and at subsonic Mach numbers the variation with sweep was similar to that predicted by theory. The results of the present investigation agreed quantitatively with the results of a free-roll investigation at subsonic Mach numbers on a series of similar wings.

Langley Aeronautical Laboratory
National Advisory Committee for Aeronautics
Langley Air Force Base, Va.

REFERENCES

1. Hammond, Alexander D.: Lateral-Control Investigation of Flap-Type Controls on a Wing with Unswept Quarter-Chord Line, Aspect Ratio 4, Taper Ratio 0.6, and NACA 65A006 Airfoil Section. Transonic-Bump Method. NACA RM L50A03, 1950.

2. Thompson, Robert F.: Lateral-Control Investigation of Flap-Type Controls on a Wing with Quarter-Chord Line Swept Back 35°, Aspect Ratio 4, Taper Ratio 0.6, and NACA 65A006 Airfoil Section. Transonic-Bump Method. NACA RM L9L12a, 1950.

3. Vogler, Raymond D.: Lateral-Control Investigation of Flap-Type Controls on a Wing with Quarter-Chord Line Swept Back 45°, Aspect Ratio 4, Taper Ratio 0.6, and NACA 65A006 Airfoil Section. Transonic-Bump Method. NACA RM L9F29a, 1949.

4. Vogler, Raymond D.: Lateral-Control Investigation of Flap-Type Controls on a Wing with Quarter-Chord Line Swept Back 60°, Aspect Ratio 4, Taper Ratio 0.6, and NACA 65A006 Airfoil Section. Transonic-Bump Method. NACA RM L50A17, 1950.

5. Polhamus, Edward C.: A Simple Method of Estimating the Subsonic Lift and Damping in Roll of Sweptback Wings. NACA TN 1862, 1949.

6. Malvestuto, Frank S., Jr., Margolis, Kenneth, and Ribner, Herbert S.: Theoretical Lift and Damping in Roll at Supersonic Speeds of Thin Sweptback Tapered Wings with Streamwise Tips, Subsonic Leading Edges, and Supersonic Trailing Edges. NACA Rep. 970, 1949.

7. Kuhn, Richard E., and Myers, Boyd C., II: Effects of Mach Number and Sweep on the Damping-in-Roll Characteristics of Wings of Aspect Ratio 4. NACA RM L9E10, 1949.

8. Lockwood, Vernard E.: Damping-in-Roll Characteristics of a 42.7° Sweptback Wing as Determined from a Wind-Tunnel Investigation of a Twisted Semispan Wing. NACA RM L9F15, 1949.

9. Edmondson, James L., and Sanders, E. Claude, Jr.: A Free-Flight Technique for Measuring Damping in Roll by Use of Rocket-Powered Models and Some Initial Results for Rectangular Wings. NACA RM L9I01, 1949.

10. Dietz, Albert E., and Edmondson, James L.: The Damping in Roll of Rocket-Powered Test Vehicles Having Rectangular Wings with NACA 65-006 and Symmetrical Double-Wedge Airfoil Sections of Aspect Ratio 4.5. NACA RM L50B10, 1950.

11. Bland, William M., Jr., and Sandahl, Carl A.: A Technique Utilizing Rocket-Propelled Test Vehicles for the Measurement of the Damping in Roll of Sting-Mounted Models and Some Initial Results for Delta and Unswept Tapered Wings. NACA RM L50D24, 1950.

12. Edmondson, James L.: Damping in Roll of Rectangular Wings of Several Aspect Ratios and NACA 65A-Series Airfoil Sections of Several Thickness Ratios at Transonic and Supersonic Speeds As Determined with Rocket-Powered Models. NACA RM L50E26, 1950.

13. MacLachlan, Robert, and Letko, William: Correlation of Two Experimental Methods of Determining the Rolling Characteristics of Unswept Wings. NACA TN 1309, 1947.

14. Donlan, Charles J., Myers, Boyd C., II, and Mattson, Axel T.: A Comparison of the Aerodynamic Characteristics at Transonic Speeds of Four Wing-Fuselage Configurations as Determined from Different Test Techniques. NACA RM L50H02, 1950.

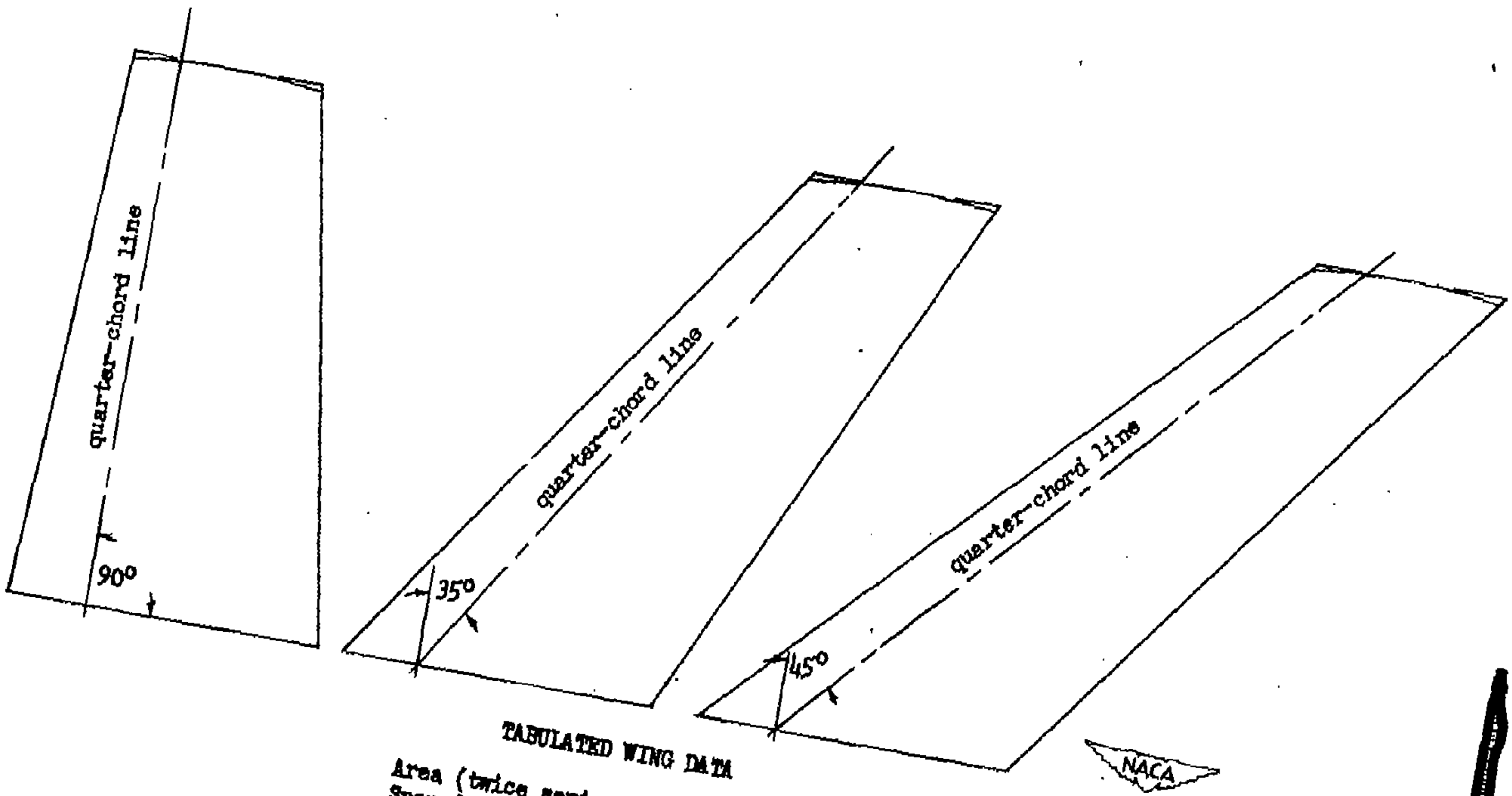

TABULATED WING DATA

Area (twice semispan)	18.00 sq.in.
Span (twice semispan)	8.486 in.
Tip chord	1.591 in.
Root chord	2.652 in.
Mean aerodynamic chord	2.166 in.
Aspect ratio	4.0
Taper ratio	0.6
Dihedral	0.0°
Incidence	0.0°
Airfoil section	NACA 65A006

Figure 1.- Three wings tested in the investigation.

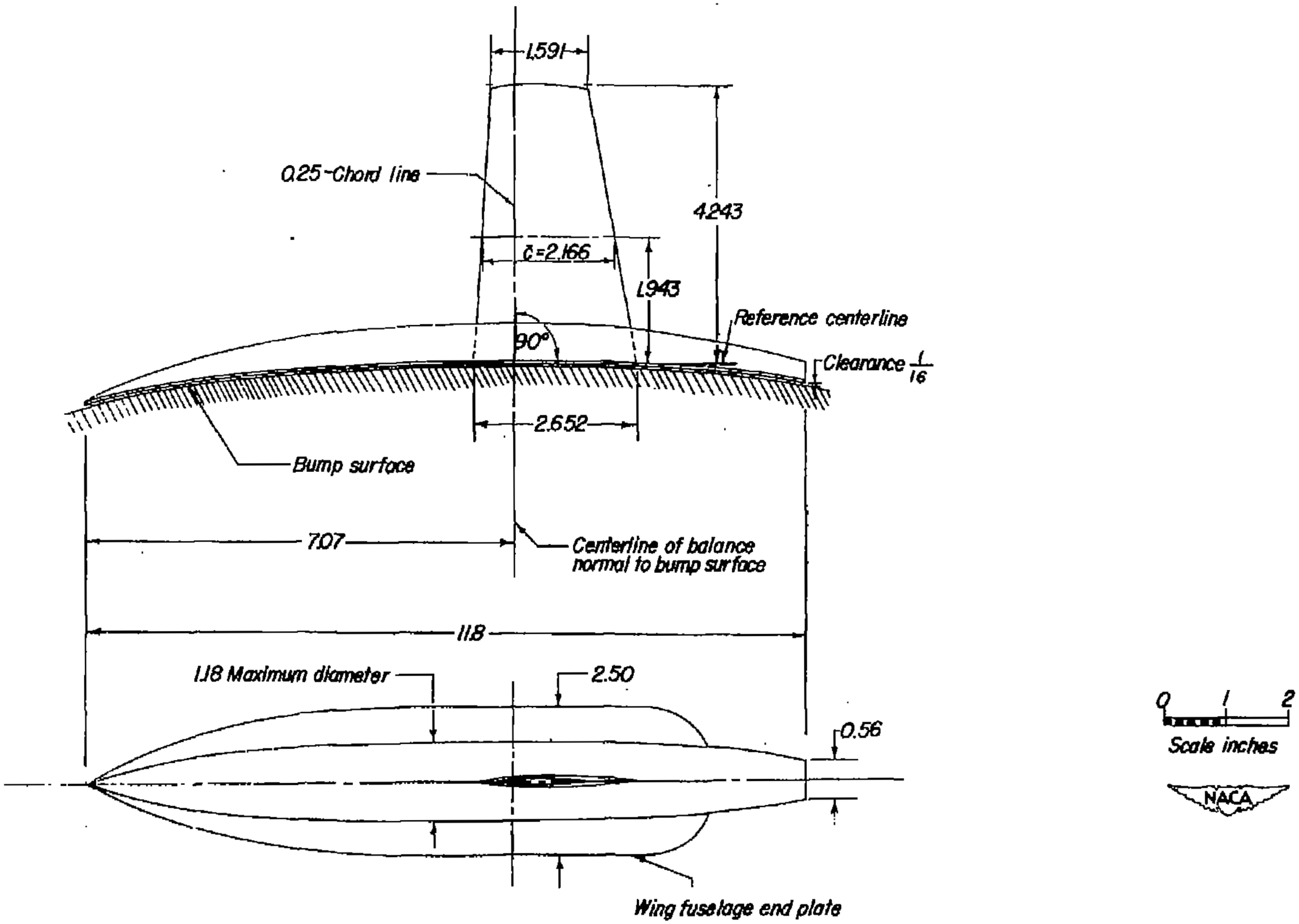

Figure 2.- General arrangement of model with 0° sweptback wing, aspect ratio 4, taper ratio 0.6, and NACA 65A006 airfoil.

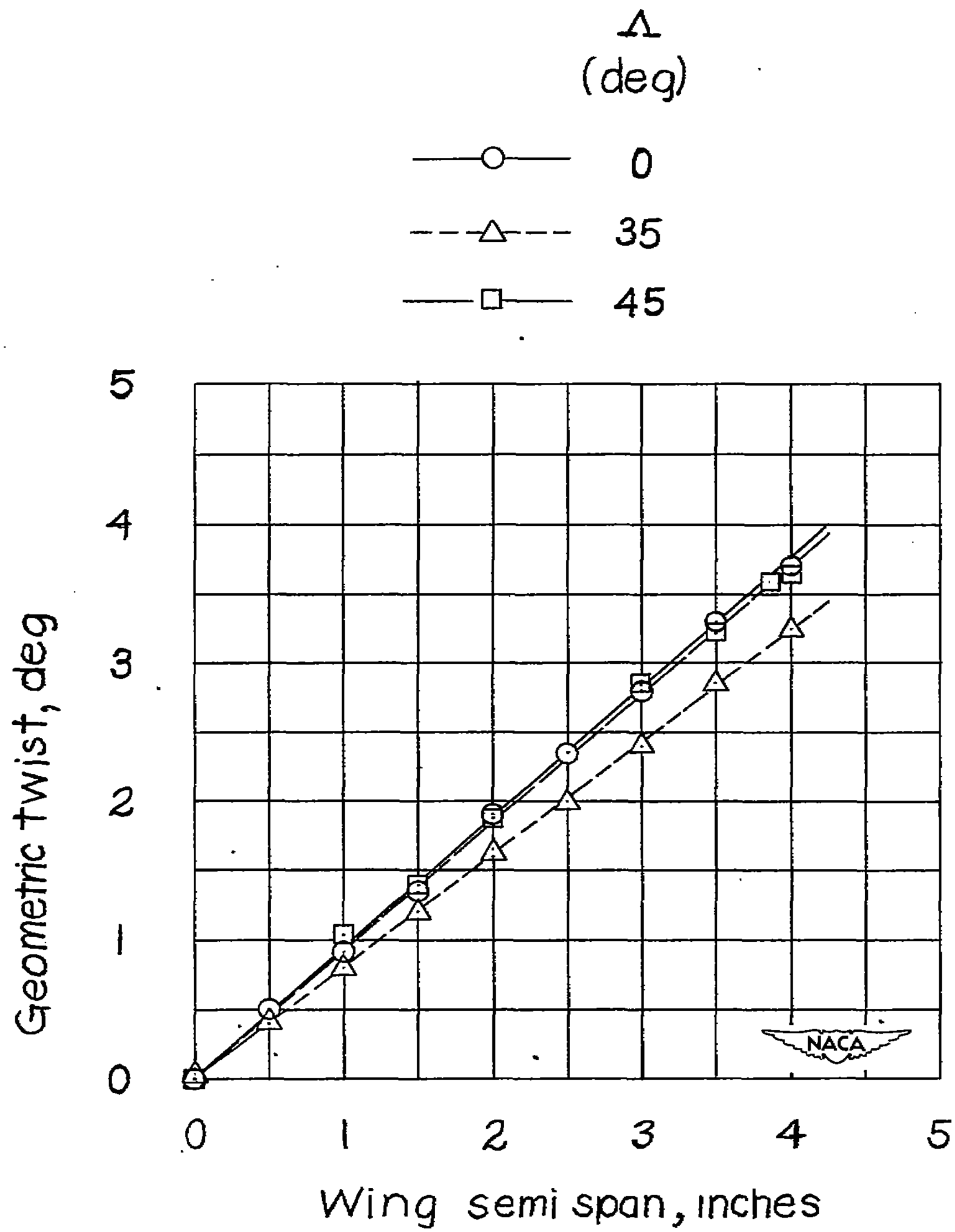

Figure 3.- Variation of geometric twist along span of models.

[redacted]

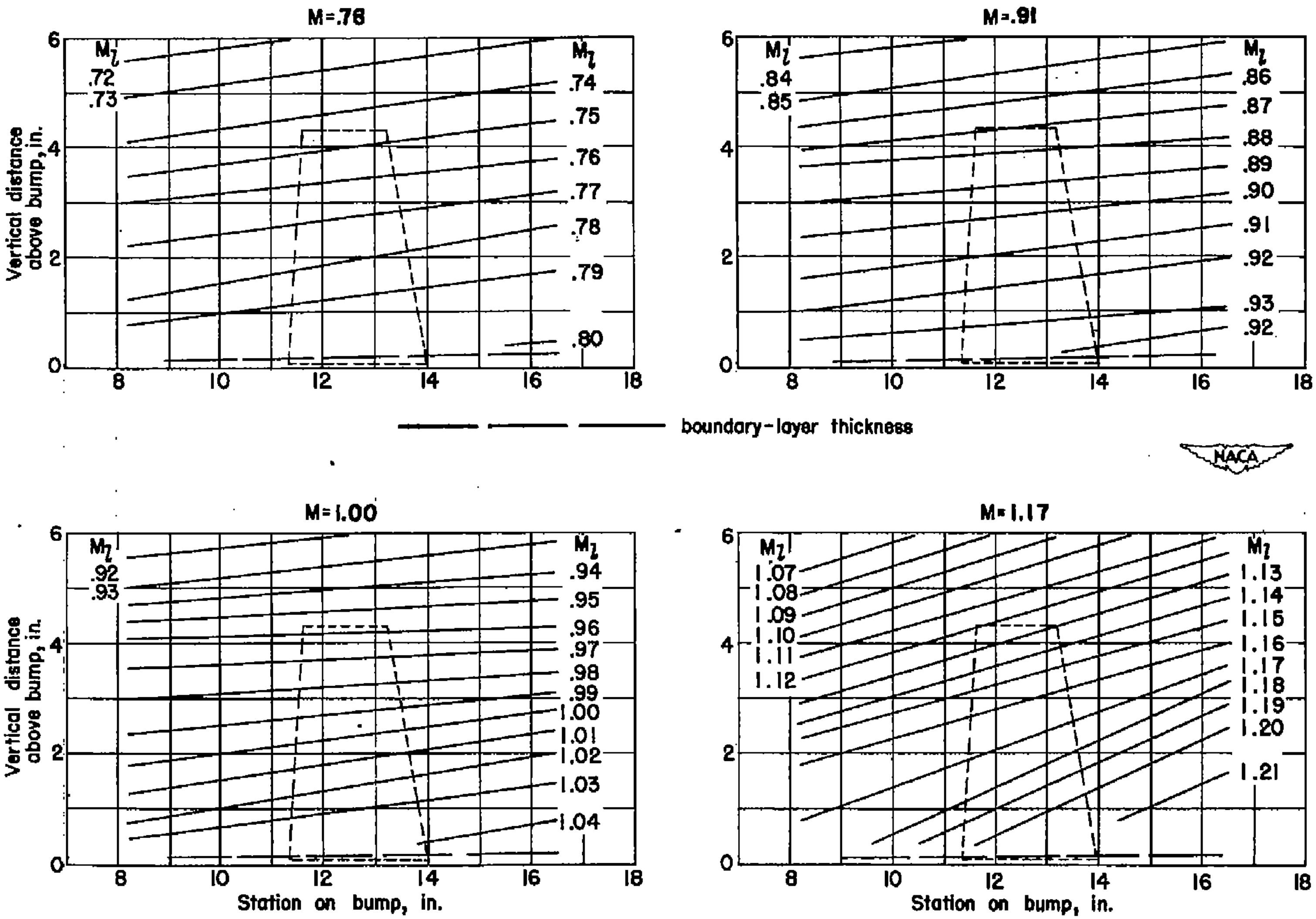

Figure 4.- Typical Mach number contours over transonic bump in region of model location.

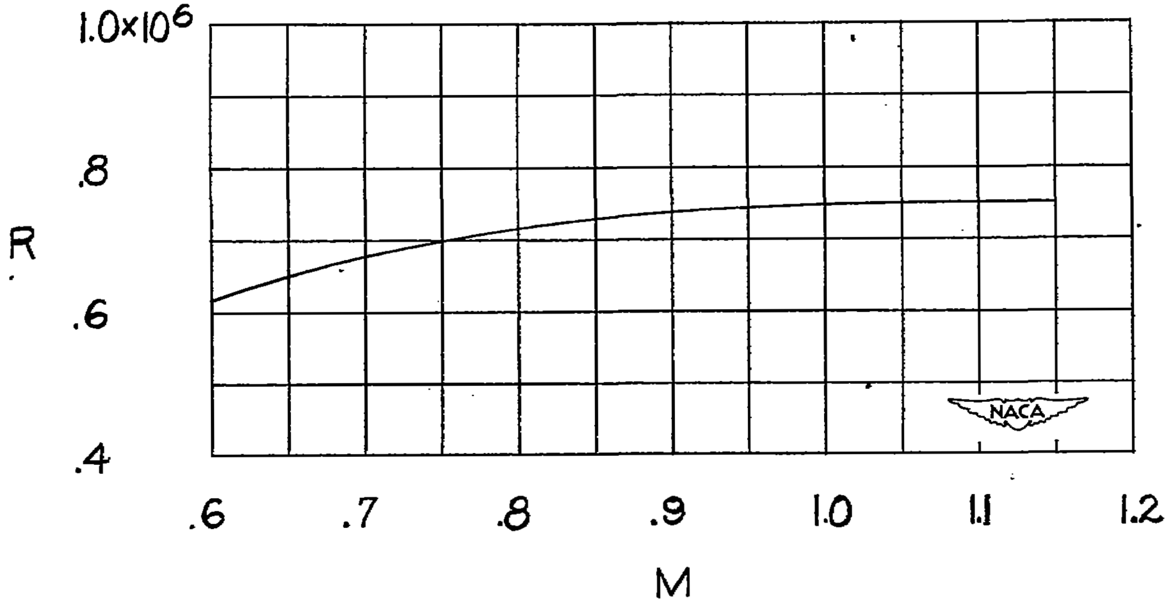

Figure 5.- Typical variation of test Reynolds number with Mach number for the models.

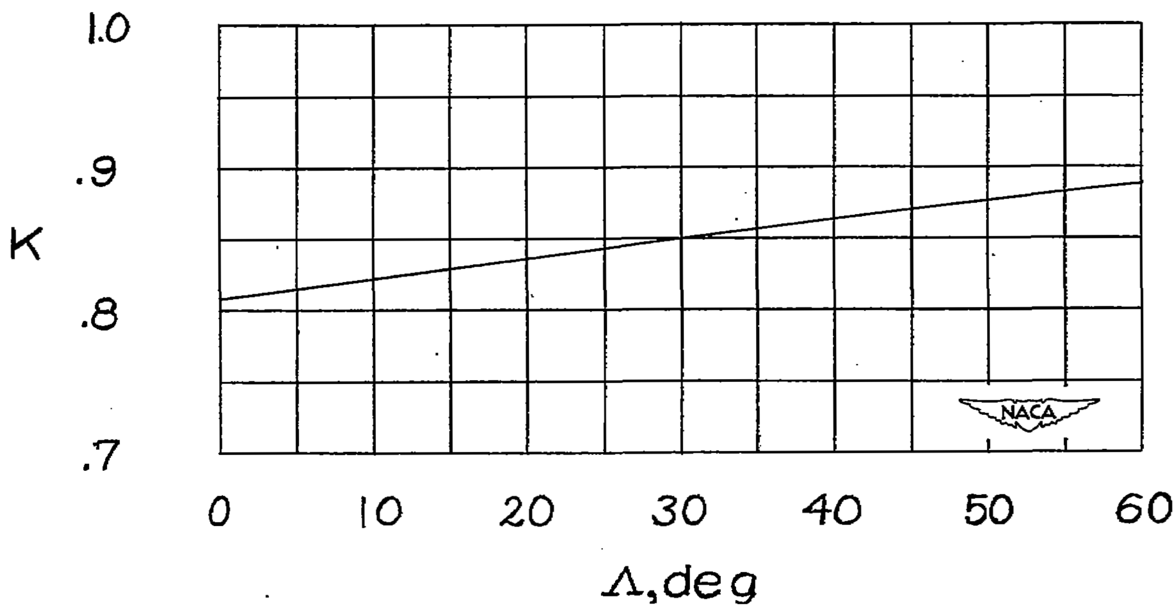

Figure 6.- Reflection-plane corrections for wings of aspect ratio 4.0, taper ratio 0.6, and having linear twist variations from root to tip.

[redacted]

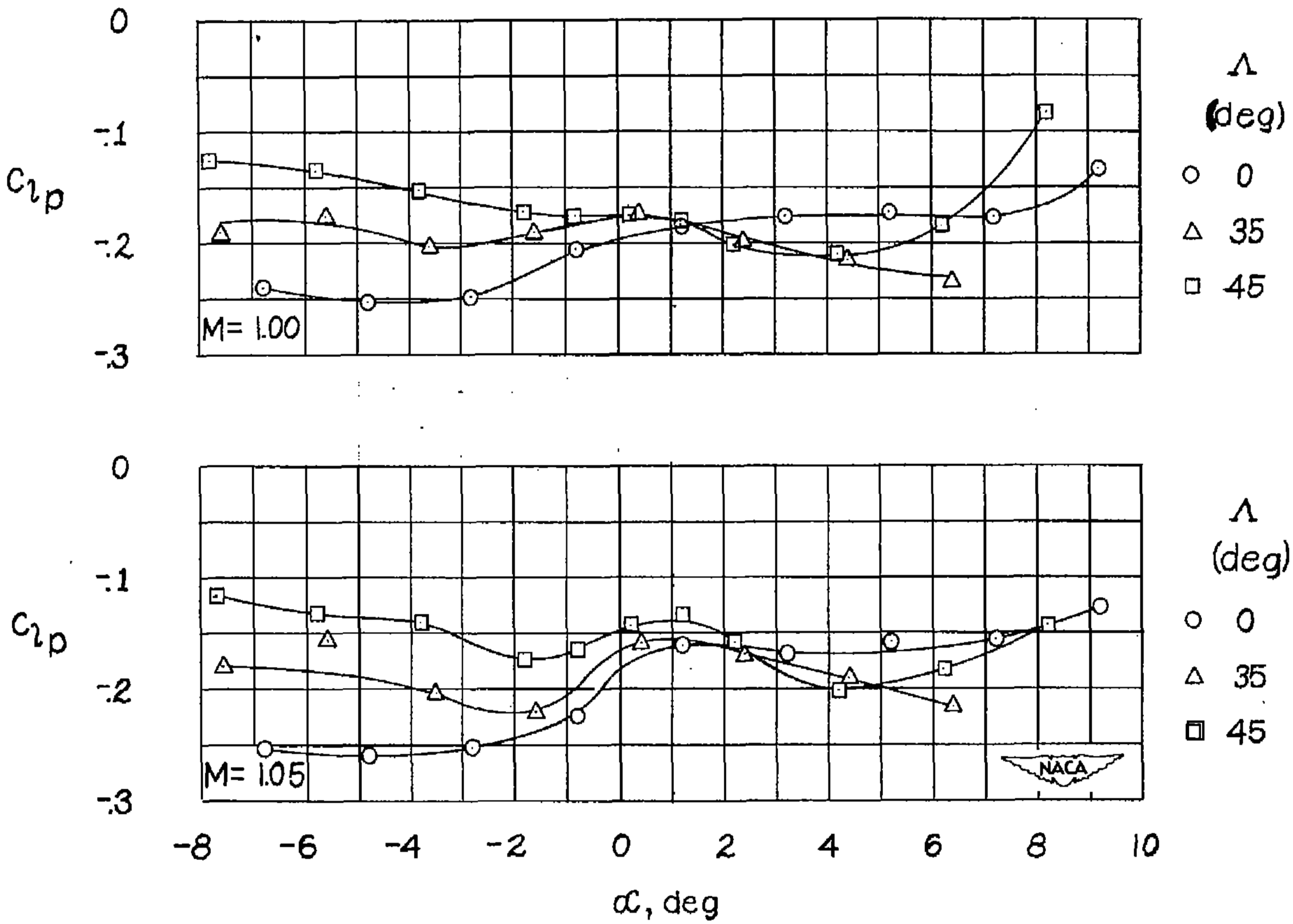

Figure 7.- Typical variations of damping-in-roll coefficient with angle of attack for a left wing.

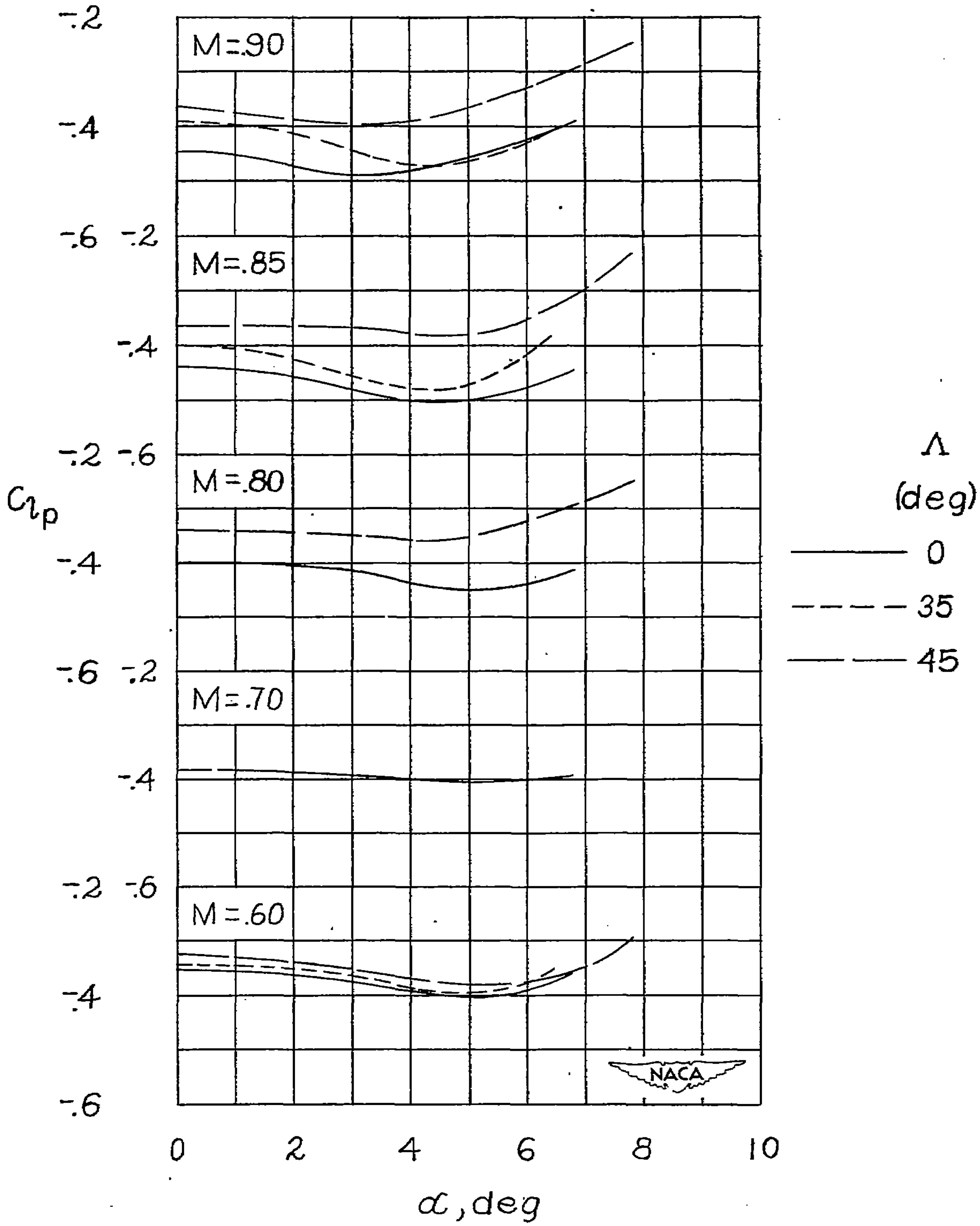

Figure 8.- Effect of angle of attack on the damping-in-roll characteristics.

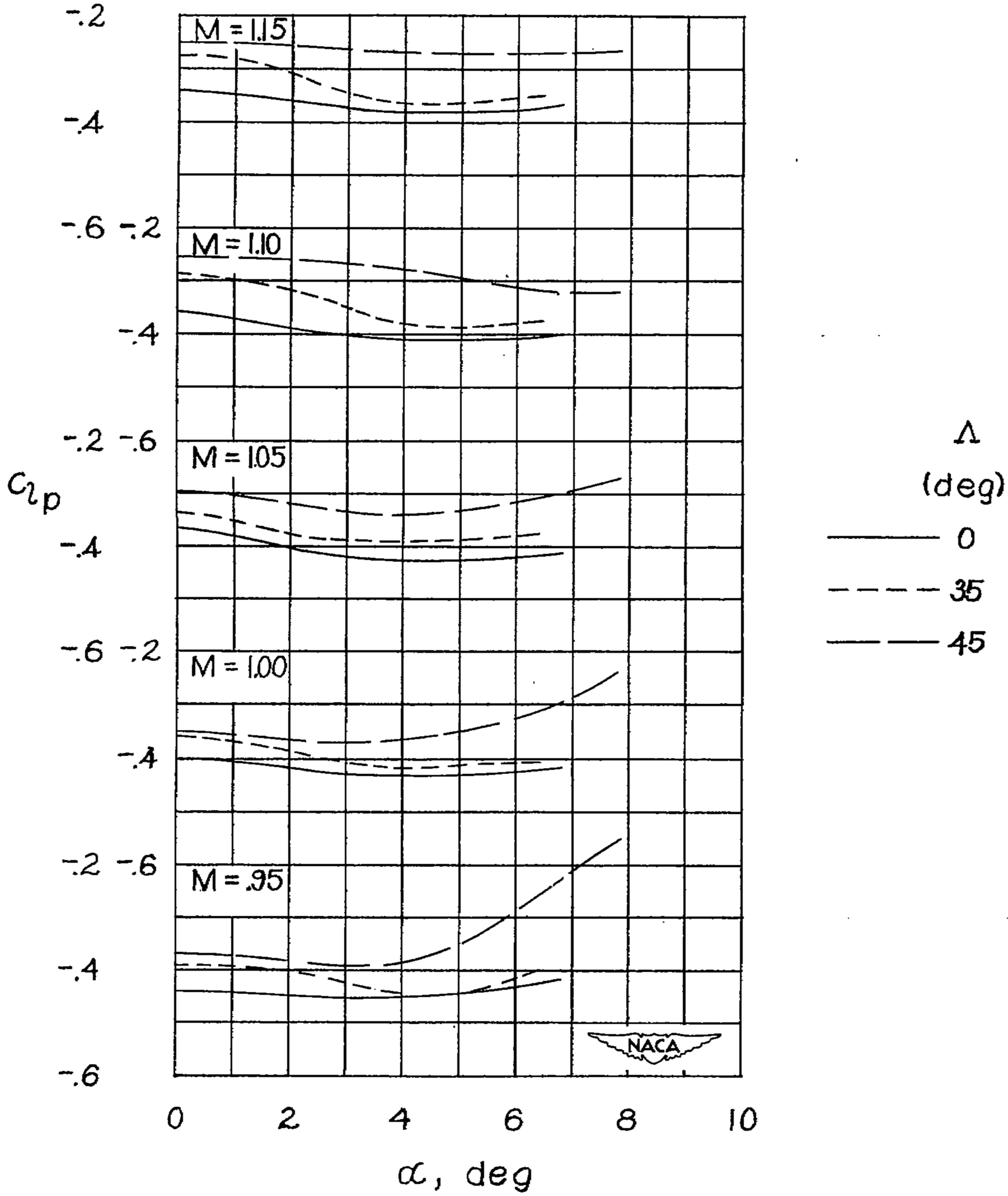

Figure 8.- Concluded.

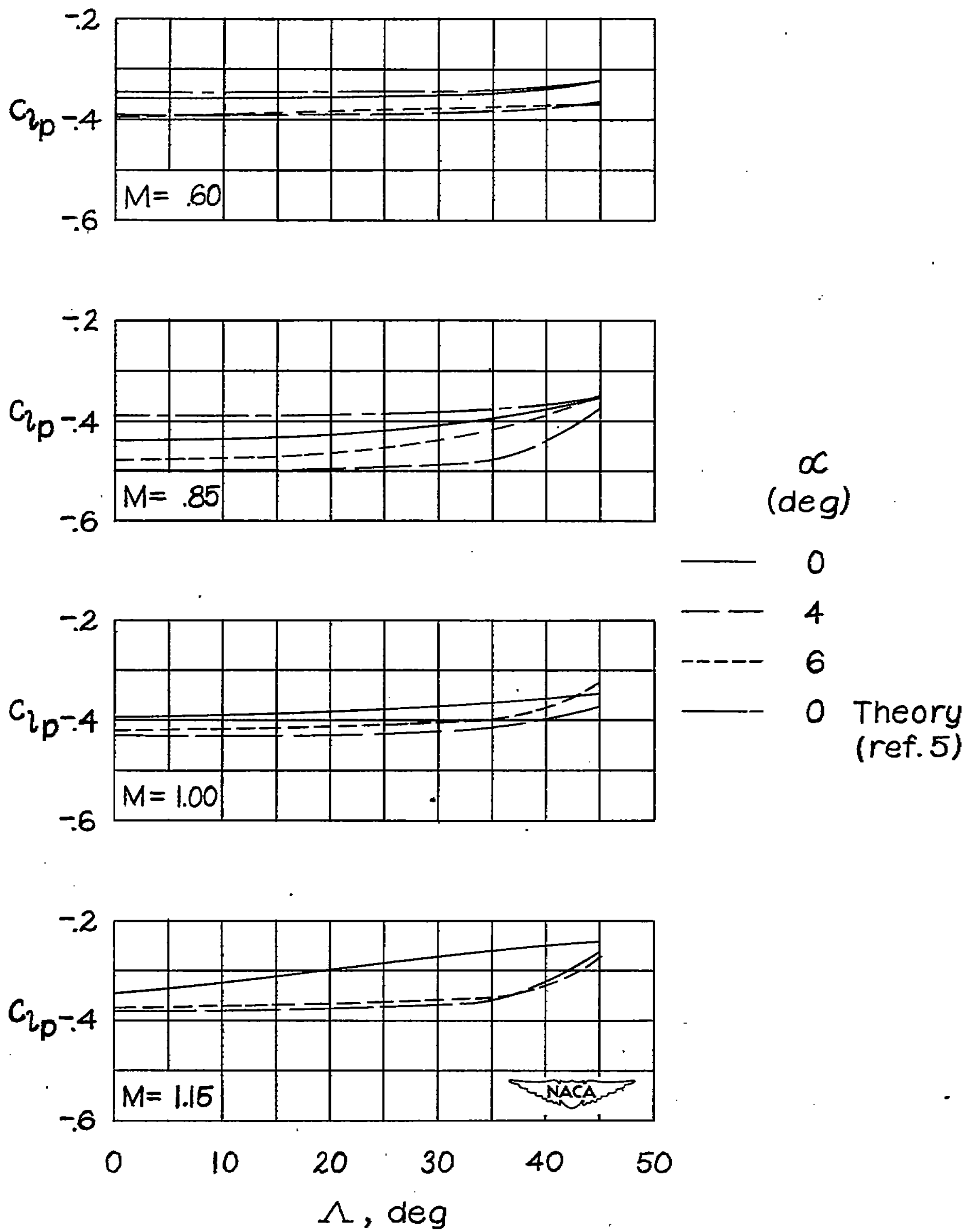

Figure 9.- Effect of angle of sweep on the damping-in-roll characteristics.

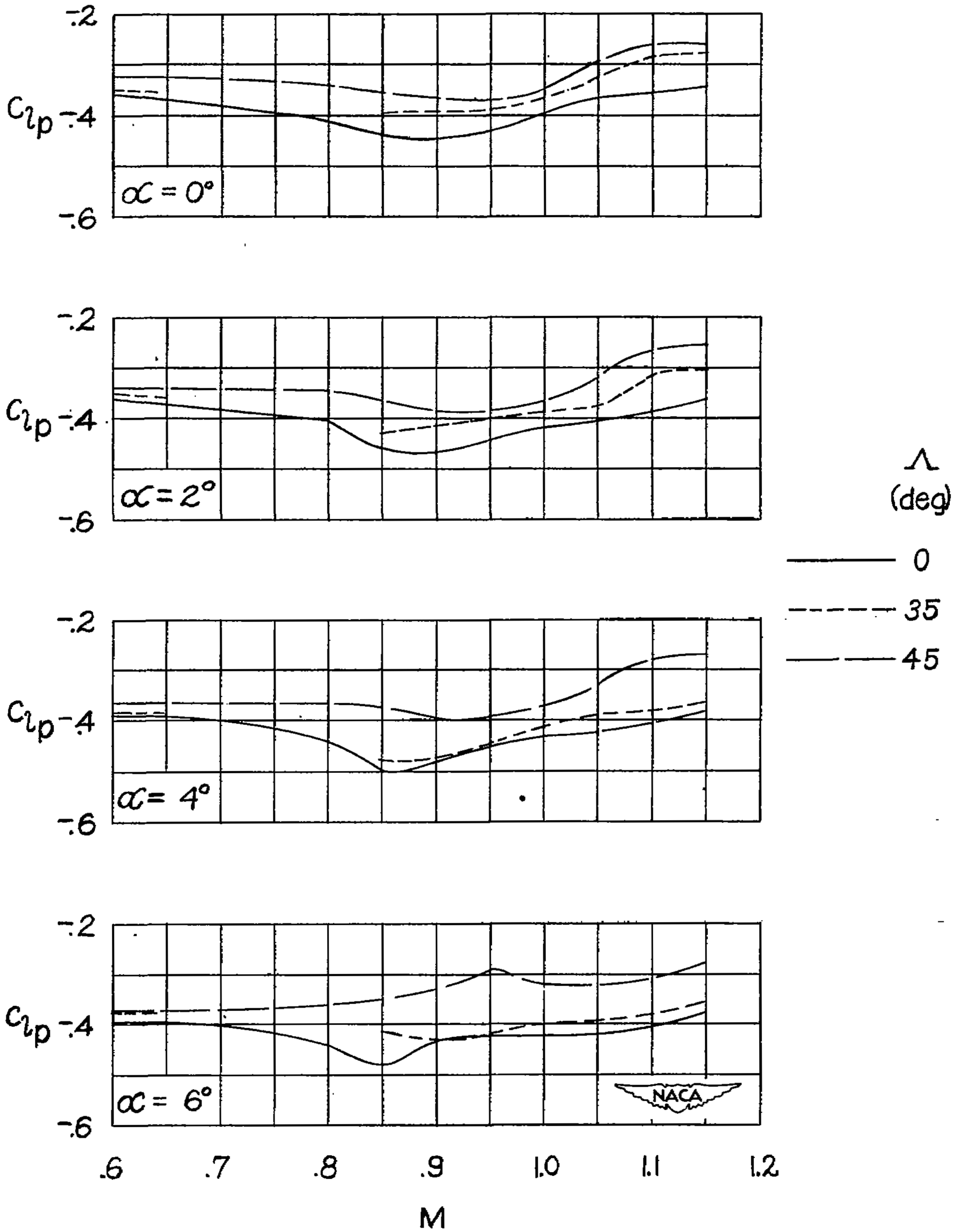

Figure 10.- Effect of Mach number on the damping-in-roll characteristics.

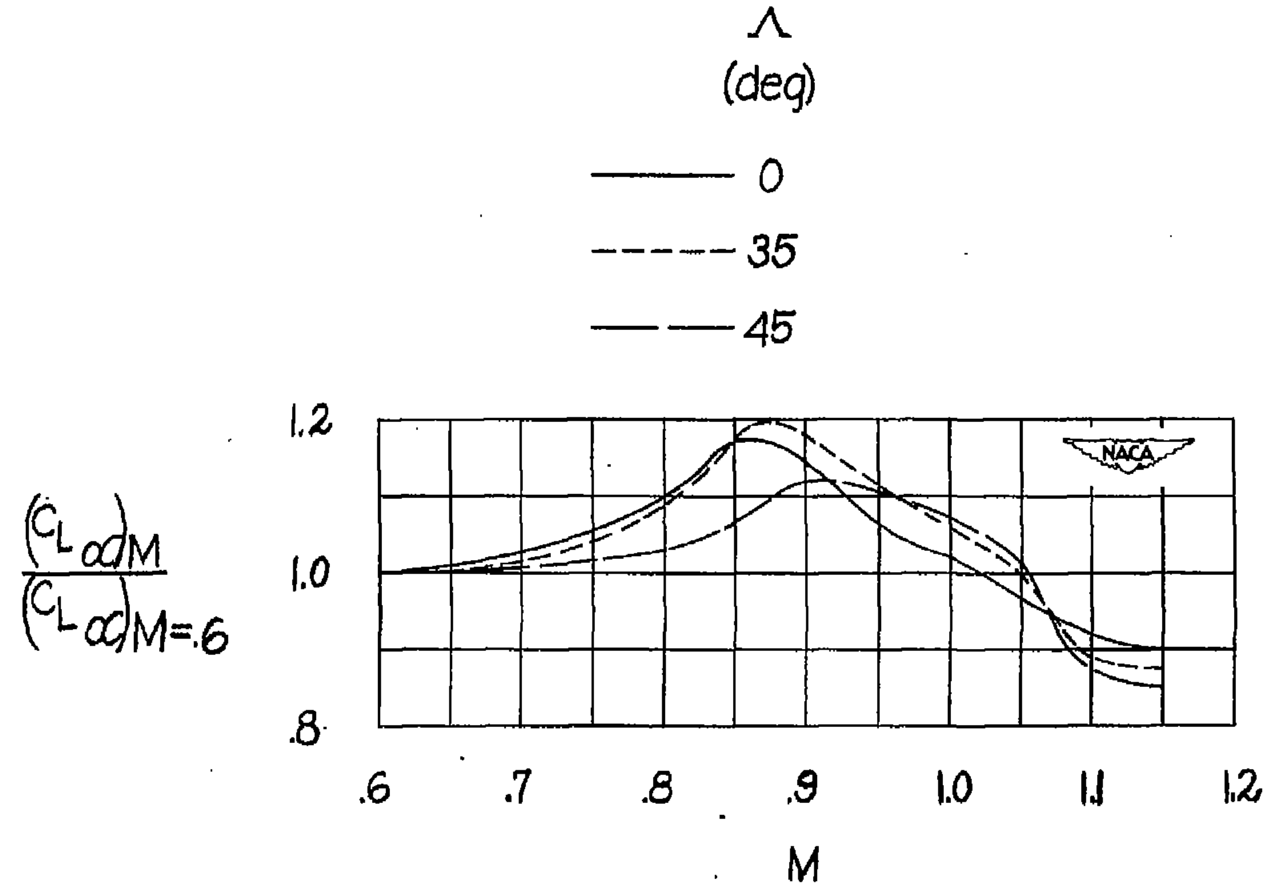

Figure 11.- Ratio of C_{L_α} at any Mach number to C_{L_α} at $M = 0.6$.

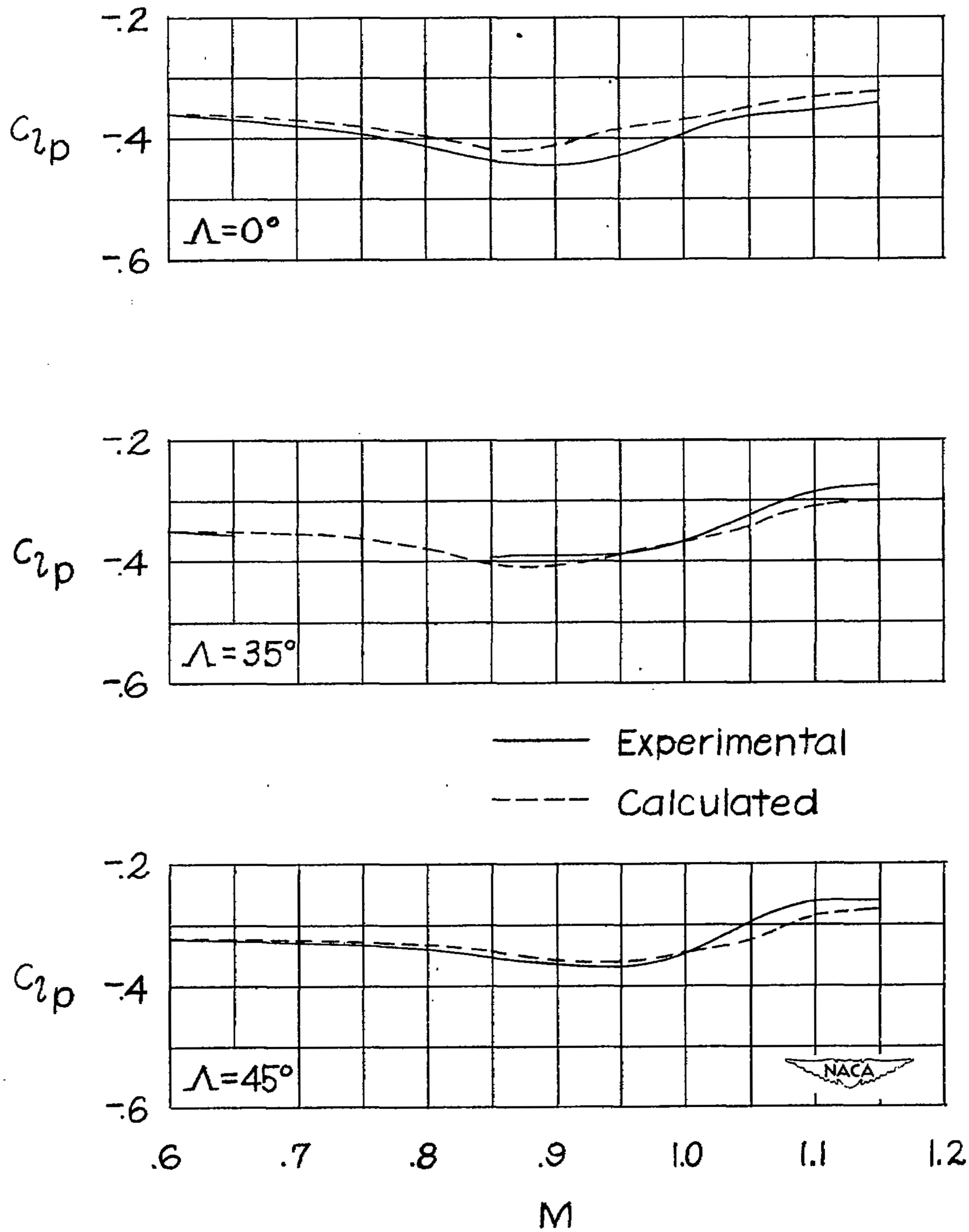

Figure 12.- Comparison of the estimated and measured damping-in-roll coefficient variation with Mach number. $\alpha = 0^{\circ}$.

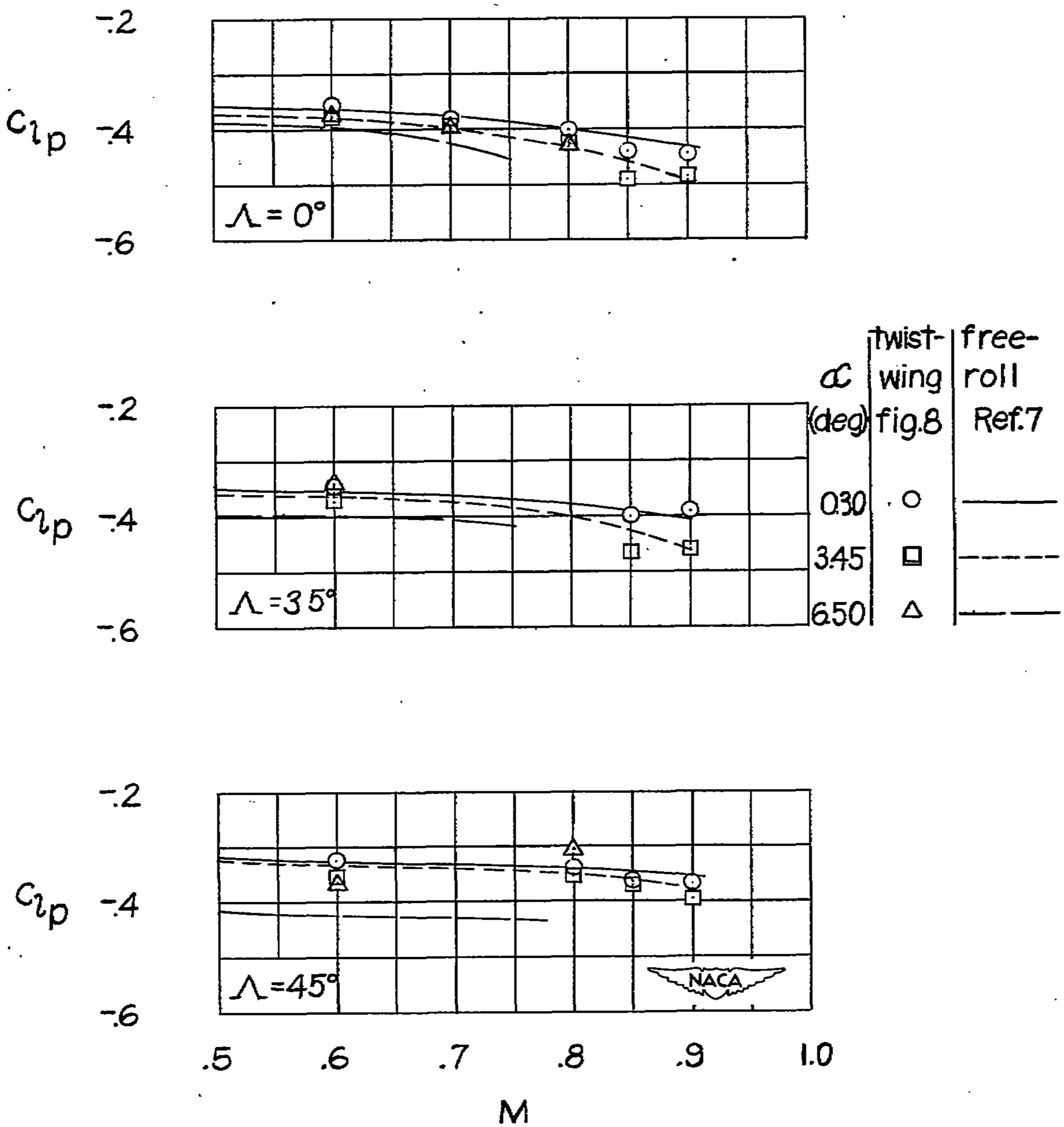

Figure 13.- Comparison of C_{l_p} obtained from the twisted-wing method and the free-roll method.

NACA-Langley - 12-14-50 - 350